JOURNAL OF SOLID STATE CHEMISTRY **139,** 225–232 (1998)
ARTICLE NO. SC987833

Zirconium Titanate from Sol–Gel Synthesis: Thermal Decomposition and Quantitative Phase Analysis

Edgardo L. Sham,* Miguel A. G. Aranda,† E. Mónica Farfan-Torres,* Juan C. Gottifredi,* María Martínez-Lara,† and Sebastián Bruque†,[1]

*INIQUI, Universidad Nacional de Salta, 177 Buenos Aires, 4400 Salta, Argentina; and †Departamento de Química Inorgánica, Cristalografía y Mineralogía, Universidad de Málaga, 29071 Málaga, Spain

Received December 2, 1997; accepted March 20, 1998

Oxides precursors $Zr_xTi_{1-x}O_2$ ($x = 0.22$, 0.39, and 0.60) were prepared by a hydrolytic sol–gel process. The amorphous mixed oxides are homogeneous as deduced from electron microscopy and XPS studies. The crystallization of these amorphous oxides was studied by TGA–DTA and thermodiffractometry. Quantitative analysis of the crystalline phases, obtained at 1000°C, was carried out by the Rietveld method. The samples are mixtures of TiO_2, $Zr_5Ti_7O_{24}$, and ZrO_2 oxides, and the stoichiometry of the stable zirconium titanate phase was found to be $Zr_5Ti_7O_{24}$ and not $ZrTiO_4$ ($=Zr_6Ti_6O_{24}$). In this work, the power of Rietveld refinements to determine phase ratios of very related (and thus very overlapped) phases is shown.

Key Words: **zirconium titanate; crystallization; quantitative Rietveld analysis; thermodiffractometry.**

INTRODUCTION

Zirconium titanate is a ceramic material widely used in electrical and optical devices such as capacitors, piezoelectric sensors, ultrasonic motors, and microwave dielectric ceramic resonators (1–4). It is also used as a refractory material, pigment, and catalyst.

This material is synthesized at very high temperature (above 1400°C) from the crystalline ceramic oxides ZrO_2 and TiO_2. However, the temperature at which the material is formed may be considerably lowered by using a sol–gel (5–7) or synthetic precursor approach (8). The size and shape of the microparticles of zirconium titanate can be controlled in sol–gel syntheses as has been reported for microfibers (9) and microspheres (10). Nonhydrolytic sol–gel processes for preparing zirconium titanate have also been published (11, 12).

$ZrTiO_4$ crystallizes in the orthorhombic α-PbO_2 type structure (13, 14). A modulated structure has also been reported in this system (15). The influence of pressure (16) and cooling rates (17) in the phase transitions in zirconium titanate has been studied. The stoichiometry of zirconium titanate depends on the synthetic conditions and the initial Zr/Ti ratio. The stoichiometries $ZrTiO_4$ (space group *Pbcn*, $a \approx 4.80$ Å, $b \approx 5.48$ Å, and $c \approx 5.03$ Å) and $Zr_5Ti_7O_{24}$ ($Zr_{0.833}Ti_{1.167}O_4$, space group *Pbcn*, $a \approx 14.36$ Å, $b \approx 5.32$ Å, and $c \approx 5.02$ Å) have been reported (18). This last unit cell is a very related supercell (a axis tripled) due to partial ordering of the metal cations. A Ti-rich zirconium titanate mineral (srinlankite) has also been reported ($Zr_{0.666}Ti_{1.334}O_4$, space group *Pbcn*, $a \approx 4.71$ Å, $b \approx 5.55$ Å, and $c \approx 5.02$ Å) (19), showing that a high titanium content is common in these phases.

Multiphase samples are important from the technological point of view. $(Zr,Ti)O_4/TiO_2$ and $(Zr,Ti)O_4/ZrO_2$ mixed materials are being widely studied and the properties of the samples stongly depend on the phase ratio and crystallinity. The main diffraction peaks of $ZrTiO_4$ and $Zr_5Ti_7O_{24}$ are well separated from those of TiO_2 (rutile structure); however, the main peaks of $ZrTiO_4$ [(111) at 2.94 Å], $Zr_5Ti_7O_{24}$ [(311) at 2.91 Å], and ZrO_2 [tetragonal structure; (101) at 2.99 Å] are strongly overlapped. Furthermore, other peaks are also overlapped and the peak positions can change slightly due to partial metal Ti/Zr substitution. These make quantitative phase analysis from single high-intensity peaks useless. In these cases, quantitative analysis using the Rietveld method (20) is much more suitable as it uses all existing diffraction peaks and is, therefore affected by fewer errors.

In this work, amorphous oxide precursors $Zr_xTi_{1-x}O_2$ are prepared by a hydrolytic sol–gel process. These initial solid are characterized by electron microscopy and XPS. The crystallization of these amorphous oxides is studied by TGA–DTA and thermodiffractometric techniques. Quantitative analysis of the high-temperature crystalline phases is carried out by the Rietveld method.

[1]To whom correspondence should be addressed.

0022-4596/98 $25.00

EXPERIMENTAL

Synthesis

To prepare the precursor gels, zirconium *n*-propoxide (ZNP) (70% in *n*-propanol) and titanium isopropoxide (TIP) (97%) were used. Gels with composition $Zr_xTi_{1-x}O_2$ ($x = 0.22, 0.39$, and 0.60) were prepared by mixing 1 M ZNP and TIP *n*-propanol solutions in the appropriate ratios and stirring for 2 hr at room temperature. Hydrolysis was then carried out by adding water dropwise up to a molar ratio $H_2O/(Zr + Ti) = 4$. The obtained gels were refluxed for 24 hr, washed, and dried at 60°C. These samples were ground to white fine powders and are named ZT22, ZT39, and ZT60, respectively (ZTsX). Firing the gels at relatively low temperatures produces the ceramic materials (ZTX). The samples for the Rietveld study were obtained by firing the ZTsX samples at 1000°C.

Characterization

TiO_2 and ZrO_2 contents were determined by X-ray fluorescence (XRF) and electron microanalysis (AEM) on samples previously calcined at 1100 and 600°C, respectively. XRF analyses were carried out on a Rigaku 2000 spectrometer. AEM measurements were made with a Philips CM 200 Supertwin-DX4 with an electron probe microanalyzer Edax (Si–Li detector). To obtain information on surface chemical composition, the samples calcined at 600°C were also studied by XPS spectrometry. XPS analyses were performed on a Physical Electronics 5700 instrument using a Mg$K\alpha$ X-ray source (1253.6 eV). Accurate (± 0.1 eV) binding energies (BE) were determined with respect to the position of the C 1*s* peak at 284.6 eV.

Thermal analyses (DTA and TGA) of the ZTsX samples were carried out in air on a Rigaku Thermoflex 8110 with a Thermal Station TAS 100 from room temperature to 1100°C at a heating rate of 10 K min^{-1} with calcined Al_2O_3 as standard reference. Powder thermodiffractometric studies of the ZTsX samples were carried out on a Siemens D-5000 diffractometer permanently equipped with an HTK10 heating chamber. The patterns were scanned over the angular range 8–38° (2θ), with a step size of 0.04° and counting time of 1 s per step. The appropriate heating and cooling temperatures were selected by using the Diffract AT software. Before any pattern was obtained, a delay time of 10 min was selected to ensure that the transformations took place. Room temperature powder diffraction patterns of the high-temperature calcined phases (ZTX) were collected in a second goniometer of the Siemens D-5000 automated diffractometer using graphite-monochromated Cu$K\alpha$ radiation. To carry out the quantitative phase analysis by the Rietveld method, data were collected between 20° and 70° (2θ) with a 0.03° step size and 3-s counting time.

TABLE 1
Positional and Thermal Parameters Used in the Quantitative Rietveld Analyses

	Site symmetry	*x*	*y*	*z*	Fraction	U_{iso} (Å^2)
"$Zr_5Ti_7O_{24}$"						
Zr	4*c*	0.00	0.2030	0.25	0.4167	0.005
Ti	4*c*	0.00	0.2030	0.25	0.5833	0.005
O	8*d*	0.2689	0.4024	0.4337	1.00	0.01
TiO_2						
Ti	2*a*	0.00	0.00	0.00	1.00	0.005
O	4*f*	0.3048	0.3048	0.00	1.00	0.01
ZrO_2						
Zr	2*b*	0.75	0.25	0.25	1.00	0.005
O	4*d*	0.25	0.25	0.4546	1.00	0.01

The powder patterns were analyzed by the Rietveld method using the GSAS (21) set of programs. The initial unit cell parameters were as follows: space group *Pbcn*, $a = 4.8$ Å, $b = 5.5$ Å, and $c = 5.0$ Å for $Zr_{0.4167}Ti_{0.5833}O_2$; space group $P4_2/mnm$, $a = 4.611$ Å, and $c = 2.982$ Å for TiO_2 (rutile structure); and space group $P4_2/nmc$, $a = 3.64$ Å, and $c = 5.27$ Å for ZrO_2 (tetragonal structure). These values were optimized in the refinement process. The atomic parameters for each phase are given in Table 1 and they were not refined.

The common overall parameters, histogram scale factor, background coefficients, zero-shift error, and pseudo-Voigt coefficients (*GW*, *LY*, and *LX*) (22) corrected for asymmetry ($H/L = 0.015$, $S/L = 0.015$) (23, 24) were refined first. Then the unit cell parameters were refined. Finally the phase ratio was optimized.

RESULTS

ZTsX samples are noncrystalline phases and they have different thermal behaviors. The chemical compositions of the samples heated at 600°C were determined by AEM and the results are reported in Table 2. AEM is a statistical

TABLE 2
Chemical Compositions of Samples Calcined at 600°C (AEM) and 1100°C (XRF)

	AEM (metal at.%)		XRF (metal at.%)	
Sample	Ti	Zr	TiO_2	ZrO_2
ZT22	77.5	22.5	76.6	23.4
ZT39	58.6	41.4	57.9	42.1
ZT60	37.8	62.2	39.1	60.9

analysis over individual microparticles. The AEM analyses show that there is no phase segregation in ZTsX solids, the compositions being very homogeneous over all particles. The chemical compositions of the samples heated at 1100°C (determined by XRF) are also presented in Table 2. The results obtained with both techniques are in good agreement, showing that the overall chemical compositions are the same at 600 and 1100°C.

XPS results are listed in Table 3. It can be seen that samples ZT22 and ZT60 present similar Zr 3*d*, Ti 2*p*, and O 1*s* BE. For ZT39, these values are shifted to higher BE. The measured BE are different from those reported in the literature for ZrO_2 (Zr $3d_{5/2} = 182.2$ eV, O $1s = 530.2$–530.9 eV) and TiO_2 (Ti $2p = 458.7 - 458.8$ eV, O $1s =$ 529.9 eV), always being shifted to lower values. Moreover, the measured BE do not correspond to those of $ZrTiO_4$ (Zr $3d_{5/2} = 182.2$ eV, Ti $2p = 458.7$–459.0 eV, O $1s = 530.2$–532.5 eV) (25). The surface chemical compositions found for all samples changes as expected from the initial molar ratios.

The differential thermal analyses in air show the presence of a very strong exothermic peak due to crystallization and/or phase transformation processes. This exotherm takes place without mass changes. The temperatures of this exotherm are 662, 700, and 690°C for ZT22, ZT39, and ZT60, respectively. These are considerably higher than that of pure ZrO_2. It has to be taken into account that these are dynamic values on heating, and therefore the true transformation temperatures have slightly lower values.

TABLE 3
Binding Energies and Surface Composition of Samples Calcined at 600°C from XPS

	Surface atoms (%)				BE (eV)		
Sample	Zr	Ti	O	O/(Zr + Ti)	Zr $3d_{5/2}$	Ti $2p_{3/2}$	O 1*s*
ZT22	8.4	21.9	69.8	2.300	181.75	458.00	529.37
ZT39	14.9	18.1	67.0	2.030	181.87	458.25	529.87
ZT60	19.7	10.7	69.7	2.300	181.75	458.00	529.37

The thermodiffractometric studies show that ZT22 crystallizes at approximately 650°C, giving TiO_2 anatase as the main component and $Zr_5Ti_7O_{24}$ (Fig. 1). The main diffraction peak of anatase is situated at 3.52 Å (25.2° 2θ), PDF no. 21-1272. After this sample was heated at 1000°C, a mixture of TiO_2 (rutile structure), $Zr_5Ti_7O_{24}$, and ZrO_2 (tetragonal structure) was observed in the XRD profile. These components were identified by their published powder patterns, PDF no. 21-1276, 34-209, and 24-1164, respectively. Due to the strong overlapping of the diffraction peaks, the phase ratio was derived from the Rietveld analysis (see later). ZT39 crystallizes near 700°C, giving mainly $Zr_5Ti_7O_{24}$ (Fig. 2).

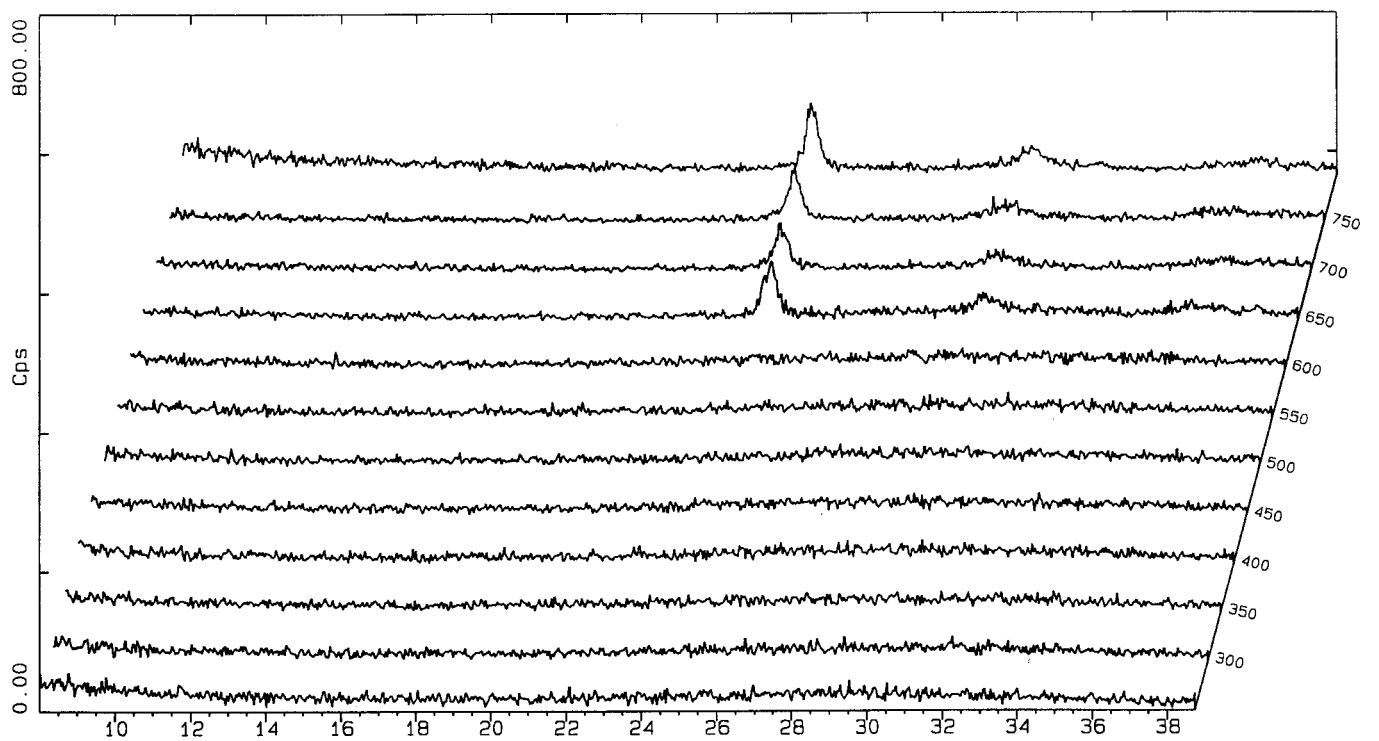

FIG. 1. X-ray thermodiffractometric powder patterns for $Zr_{0.22}Ti_{0.78}O_2$ (ZT22).

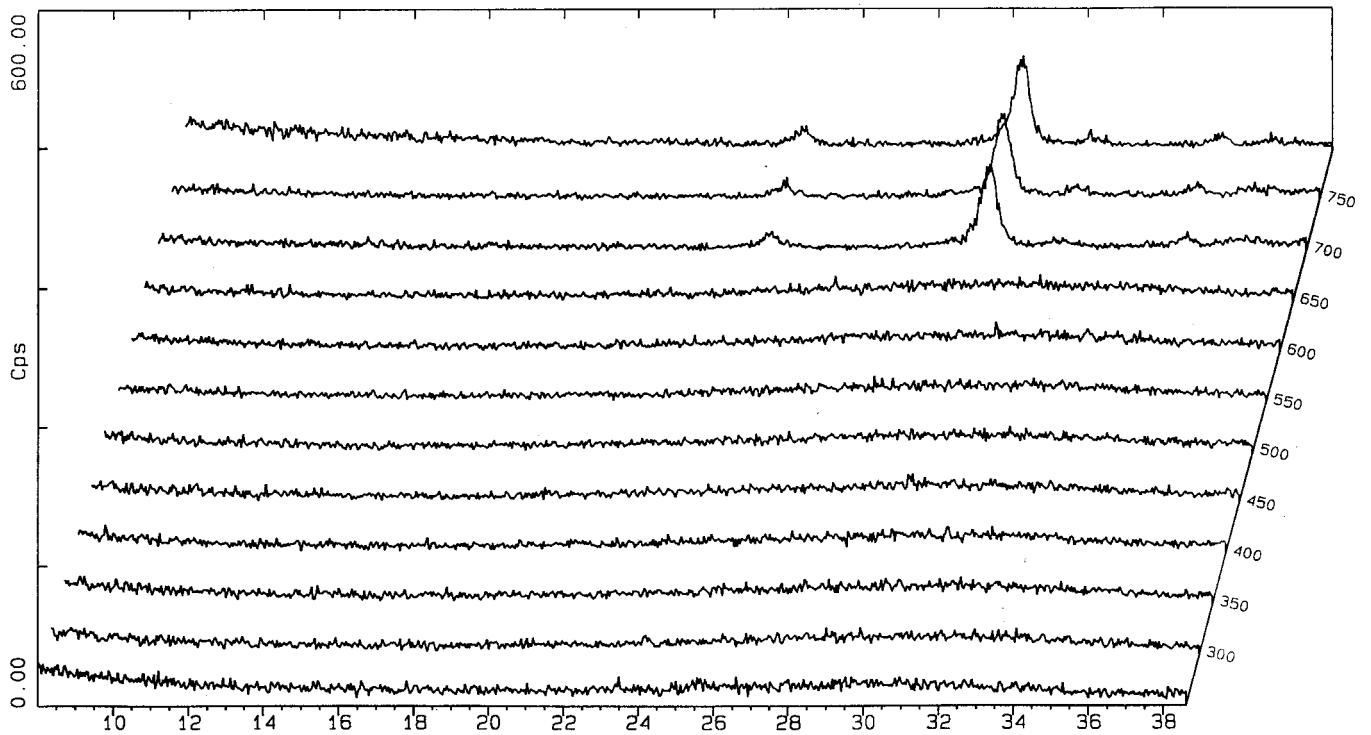

FIG. 2. X-ray thermodiffractometric powder patterns for $Zr_{0.39}Ti_{0.61}O_2$ (ZT39).

However, a detailed study of the powder pattern of the sample calcined at 1000°C reveals the presence of a tiny amount of rutile. ZT60 crystallization starts at 650°C and it is finished at 700°C (Fig. 3). From the medium-resolution thermodiffractometric study, only the $Zr_5Ti_7O_{24}$ phase is evident, as ZrO_2 peaks are overlapped down to the $Zr_5Ti_7O_{24}$ major peaks.

The power of the Rietveld method in carrying out a quantitative phase analysis of multiphase samples with strong overlapping is evidenced in this study. The results of the phase analysis are shown in Tables 4 and 5. Table 4 shows the determined weight phase fractions together with the calculated weight fractions derived from the initial composition of the samples (corroborated with the chemical analysis). However, we point out that ZT22 heated at 1000°C is a triphasic sample with TiO_2, $Zr_5Ti_7O_{24}$, and ZrO_2. Thus, it is not possible to calculate the theoretical final composition that will yield $Zr_{0.22}Ti_{0.78}O_2$. To compare the refined values with "some" calculated, we *assumed* that the final calculated rutile composition was 63.9% and then derived the phase fractions for $Zr_5Ti_7O_{24}$ and ZrO_2. Table 5 shows the refined unit cell and peak shape parameters. The final Rietveld plots are shown in Figs. 4, 5, and 6 for ZT22, ZT39, and ZT60, respectively. R_{wp} ranges between 18 and 22% and R_p ranges between 14 and 16% for the three refined patterns.

DISCUSSION

The exothermic peak observed in the DTA can be related to the different phase compositions of the ZTsX samples. For ZT22, the exothermic peak at 662°C is very sharp and strong and is due to the crystallization of the amorphous precursor. It must be mainly related to the formation of $Zr_5Ti_7O_{24}$ because TiO_2 anatase crystallization takes place with minor changes in the DTA. The strong exotherm at 700°C for ZT39 also corresponds to the crystallization of zirconium titanate, in agreement with the DTA results

TABLE 4
Quantitative Crystalline Phase Analysis by the Rietveld Method

Sample	Phases	Weight fraction (%)		Determined overall molar ratio
		Calculated	Determined	
$Zr_{0.22}Ti_{0.78}O_2$	TiO_2	64.3 (fixed)	64.3	$Zr_{0.173}Ti_{0.827}O_2$
	$Zr_5Ti_7O_{24}$	24.4	23.7	
	ZrO_2	11.3	12.0	
$Zr_{0.39}Ti_{0.61}O_2$	TiO_2	5.3	2.9	$Zr_{0.402}Ti_{0.598}O_2$
	$Zr_5Ti_7O_{24}$	94.7	97.1	
$Zr_{0.60}Ti_{0.40}O_2$	$Zr_5Ti_7O_{24}$	63.4	61.3	$Zr_{0.612}Ti_{0.388}O_2$
	ZrO_2	36.6	38.7	

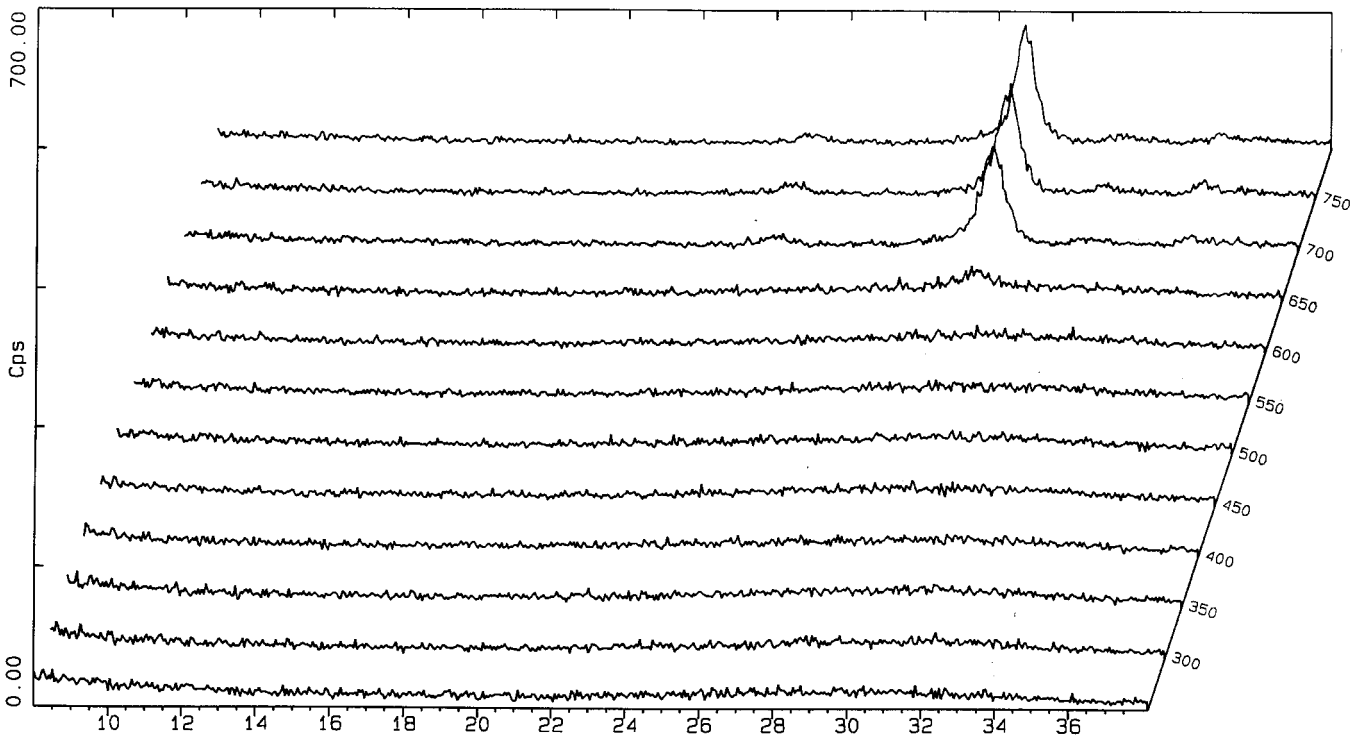

FIG. 3. X-ray thermodiffractometric powder patterns for $Zr_{0.60}Ti_{0.40}O_2$ (ZT60).

reported for gels prepared by hydrolysis of metal alkoxides (26). For ZT60, the exothermic change takes place at 690°C.

The thermodiffractometric study indicates that the samples calcined at 600°C are amorphous, and the AEM and XPS studies confirm that they are mixed oxides. The samples cannot also be a mixture of amorphous oxides or $ZrTiO_4$ because the Ti 2*p* and Zr 3*d* measured BE do not correspond to those of either the isolated oxides or $ZrTiO_4$. Upon crystallization, phase segregation takes place as shown by thermodiffractometry.

The refined phase ratios (Table 4) are in good agreement with those expected from the initial compositions. Average errors of the order of 2% have been found in this study, which are low taking into account the large overlapping between diffraction peaks worsened by the broad peaks shown by some phases. We emphasize that the stoichiometry found for the zirconium titanate phase is invariably $Zr_5Ti_7O_{24}$. If the Rietveld refinements are carried out with the stoichiometry $ZrTiO_4$, for zirconium titanate, R_{wp} only worsens (increases) by 0.5% but the determined phase ratios make no sense.

Quantitative phase analysis by the Rietveld method requires stoichiometric phases for the simulation of the theoretical profiles. As shown by the unit cell values of TiO_2 (Table 5), this phase is very crystalline (sharp peaks), with the refined unit cell parameters very close to those reported

TABLE 5
Refined Unit Cell and Peak Shape Parameters for the Final Rietveld Refinements

Sample	Phases	*a* (Å)	*b* (Å)	*c* (Å)	*V* (Å^3)	*LY* (deg)
$Zr_{0.22}Ti_{0.78}O_2$	TiO_2	4.6118(3)	4.6118	2.9817(2)	63.42(1)	0.058(16)[a]
	$Zr_5Ti_7O_{24}$	4.800(4)	5.457(4)	5.027(4)	131.7(1)	1.48(7)
	ZrO_2	3.571(1)	3.571	5.224(2)	66.60(3)	0.88(4)
$Zr_{0.39}Ti_{0.61}O_2$	TiO_2	4.6114	4.6114	2.9817	63.41	0.53(1)
	$Zr_5Ti_7O_{24}$	4.765(1)	5.473(1)	5.018(1)	130.85(7)	1.02(1)
$Zr_{0.60}Ti_{0.40}O_2$	$Zr_5Ti_7O_{24}$	4.862(3)	5.403(3)	5.033(3)	132.2(1)	1.59(5)
	ZrO_2	3.558(2)	3.558	5.262(3)	66.62(7)	1.76(5)

[a] *LX* was also refined: 0.071(5)°.

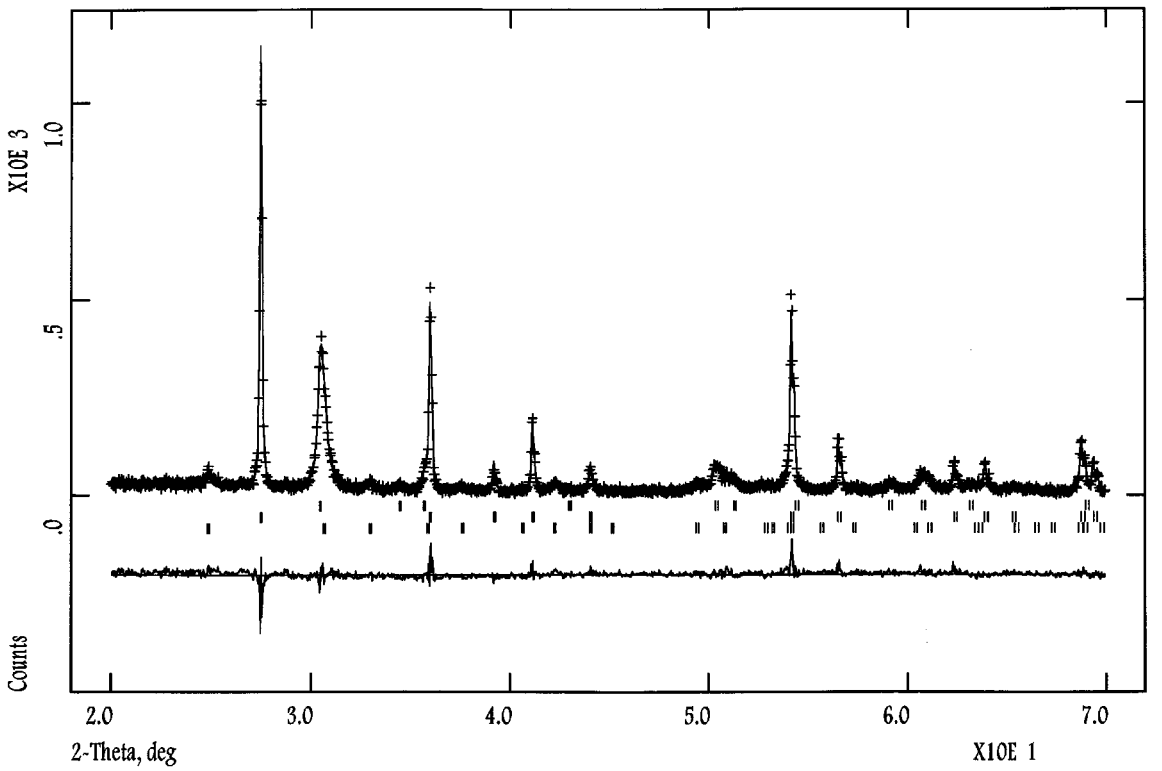

FIG. 4. Observed, calculated, and difference X-ray diffraction plots for $Zr_{0.22}Ti_{0.78}O_2$ (ZT22) calcined at 1000°C. Reflection positions for $Zr_5Ti_7O_{24}$ (bottom), TiO_2 (center), and ZrO_2 (top) are marked.

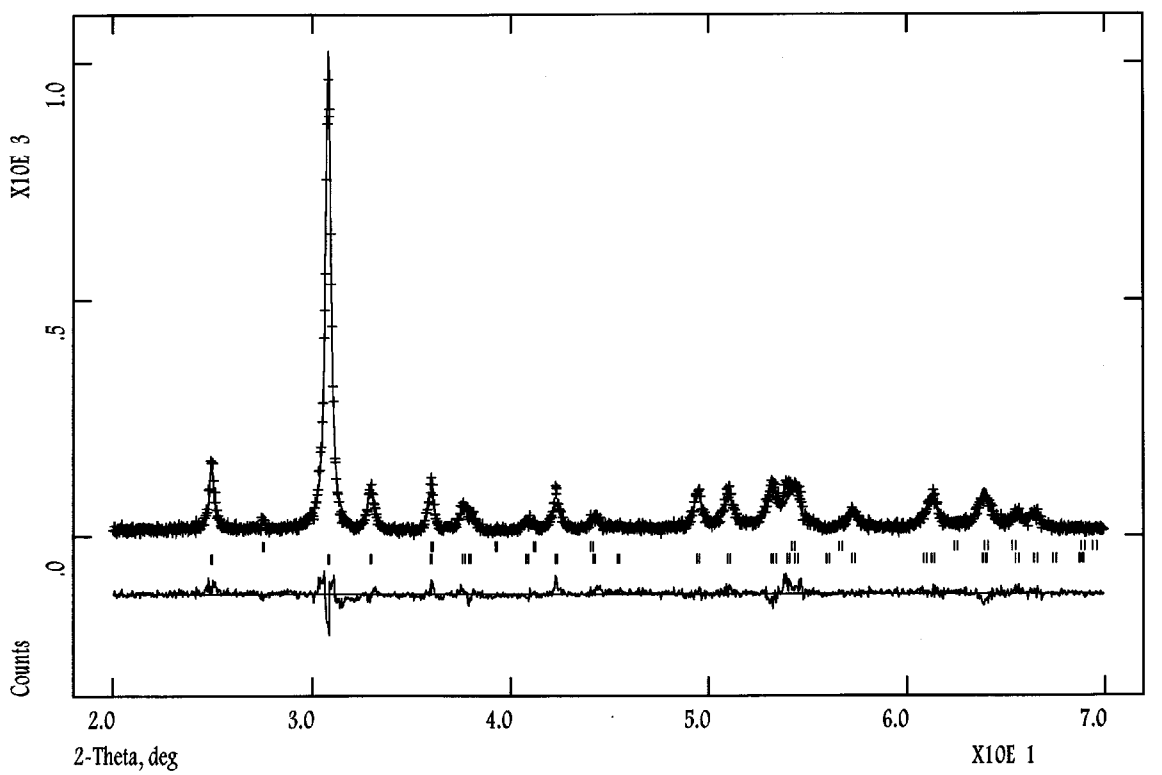

FIG. 5. Observed, calculated, and difference X-ray diffraction plots for $Zr_{0.39}Ti_{0.61}O_2$ (ZT39) calcined at 1000°C. Reflection positions for $Zr_5Ti_7O_{24}$ (bottom) and TiO_2 (top) are marked.

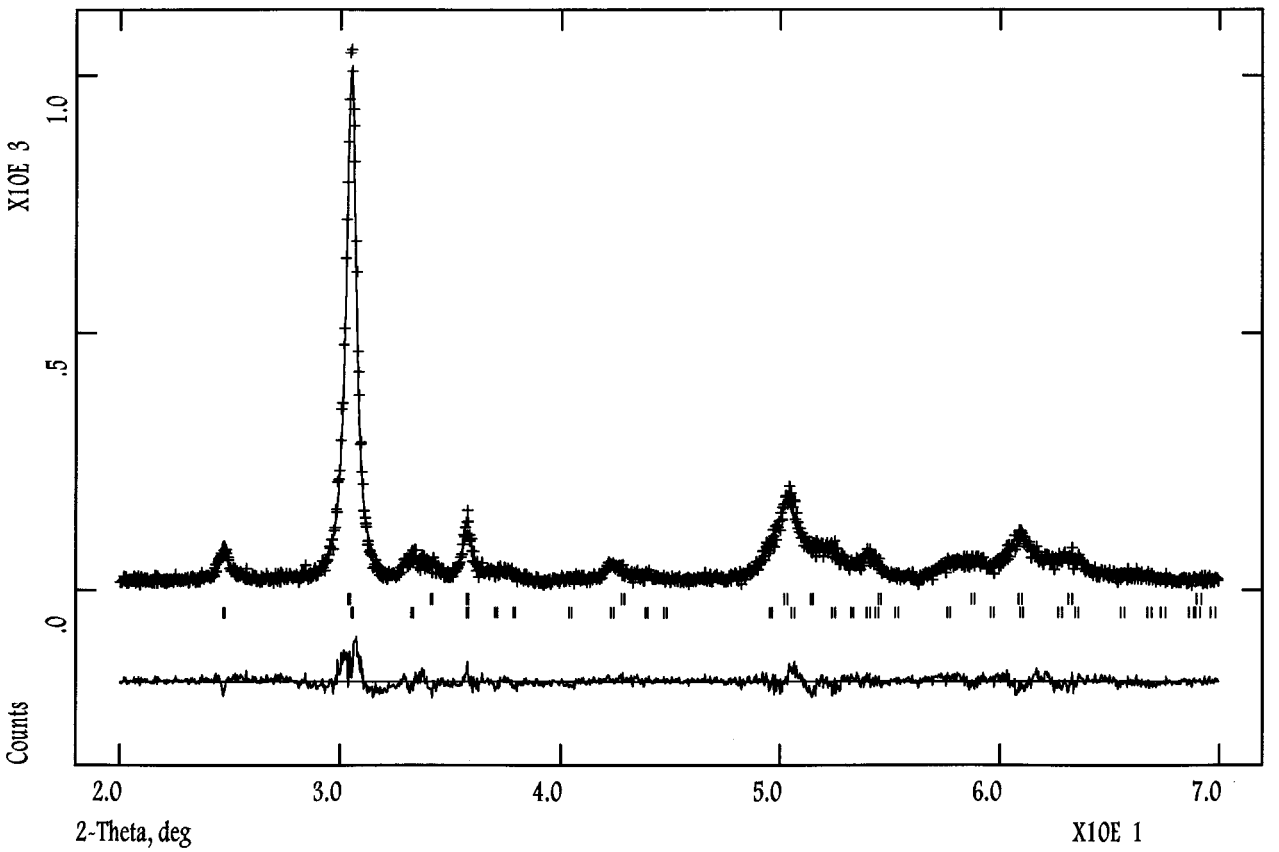

FIG. 6. Observed, calculated, and difference X-ray diffraction plots for $Zr_{0.60}Ti_{0.40}O_2$ (ZT60) calcined at 1000°C. Reflection positions for $Zr_5Ti_7O_{24}$ (bottom) and ZrO_2 (top) are marked.

in the literature. However, some slight deviations from stoichiometry may occur for $Zr_5Ti_7O_{24}$ and ZrO_4 (tetragonal). As shown in Table 5, the refined volumes of these phases show some small variations. This implies some errors in the refined compositions that would explain the slight disagreement between starting and refined compositions. Furthermore, the presence of amorphous oxides is not taken into account by this type of Rietveld analysis. However, the close relationship between the overall starting compositions and the overall refined metal ratios suggests that amorphous phases are negligible in these systems.

Finally, we emphasize that the peak shapes vary considerably for different phases and samples. For a given firing temperature, zirconium-rich phases show broader peaks. ZT60 heated at 1000°C presents very broad peaks (Fig. 6, Table 5) due to lattice microstrain rather than microparticle-related broadening. This is due to some local deviation from ideal stoichiometry in the microcrystallites.

ACKNOWLEDGMENTS

The cooperation between Málaga and Salta has been financed by AECI through the "Programa de Cooperación con Iberoamérica (Ministerio de Asuntos Exteriores, España)." This work was also supported by research grant FQM-113 from the Junta de Andalucía (Málaga) and the PID-BID CONICET IO-305 Project (Salta).

REFERENCES

1. C. L. Wang, H. Y. Lee, F. Azough, and R. Freer, *J. Mater. Sci.* **32,** 1693 (1997).
2. K. Okuyama, S. Kawashima, and K. Kugimya, Patent JP 95-156198, JP-09002871, 1997.
3. Y. K. Park and H. G. Kim, *Solid State Commun.* **102,** 565 (1997).
4. S. Yamagushi, K. Kobayashi, Y. Igushi, N. Yamada, and T. Kato, *Jpn. J. Appl. Phys.* **33,** 5471 (1994).
5. J. A. Navio, F. J. Marchena, M. Macias, P. J. Sanchez-Soto, and P. Pichat, *J. Mater. Sci.* **27,** 2463 (1992).
6. J. A. Navio, F. J. Marchena, M. Macias, P. J. Sanchez-Soto, and P. Pichat, *J. Therm. Anal.* **40,** 1095 (1993).
7. A. K. Bhattacharya, K. K. Mallick, A. Hartridge, and J. L. Woodhead, *Mater. Lett.* **18,** 247 (1994).
8. M. M. A. Sekar and K. C. Patil, *Mater. Res. Bull.* **28,** 485 (1993)
9. A. K. Bhattacharya, A. Hartridge, K. K. Balik, and D. Taylor, *J. Mater. Sci.* **31,** 5583 (1996).
10. A. K. Bhattacharya, K. K. Mallick, A. Hartridge, and J. L. Woodhead, *J. Mater. Sci.* **31,** 267 (1996).
11. M. Adrianainarivelo, R. J. P. Corriu, D. Leclercq, P. H. Mutin, and A. Vioux, *J. Sol–Gel Sci. Technol.* **8,** 89 (1997).

12. M. Adrianainarivelo, R. J. P. Corriu, D. Leclercq, P. H. Mutin, and A. Vioux, *J. Mater. Chem.* **7,** 279 (1997).
13. R. E. Newnham, *J. Am. Ceram. Soc.* **50,** 216 (1967).
14. A. Siggel and M. Jansen, *Z. Anorg. Allg. Chem.* **582,** 93 (1990).
15. A. Yamamoto, T. Yamada, H. Ikawa, O. Fukunaga, K. Tanaka, and F. Marumo, *Acta Crystallogr., Sect. C* **47,** 1588 (1991).
16. Y. K. Park, H. G. Kim, and Y. H. Kim, *Jpn. J. Appl. Phys. Lett.* **35,** L1198 (1996).
17. Y. K. Park, Y. H. Kim, and H. G. Kim, *Ferroelectr. Lett.* **21,** 65 (1996).
18. P. Bordet, A. McHale, A. Santoro, and R. S. Roth, *J. Solid State Chem.* **64,** 30 (1986).
19. A. Willgallis and H. Hartl, *Z. Kristallogr.* **164,** 59 (1983).
20. H. M. Rietveld, *J. Appl. Crystallogr.* **2,** 65 (1969).
21. A. C. Larson and R. B. Von Dreele, Los Alamos National Laboratory Report No. LA-UR-86-748, (1994).
22. P. Thompson, D. E. Cox, and J. B. Hasting, *J. Appl. Crystallogr.* **20,** 79 (1987).
23. L. W. Finger, D. E. Cox, and A. P. Jephcoat, *J. Appl. Crystallogr.* **27,** 892 (1994).
24. M. A. G. Aranda, A. Cabeza, E. R. Losilla, and S. Bruque, *J. Appl. Crystallogr.* **31,** 16 (1998).
25. H. Ikawa, T. Yamada, K. Kojima, and S. Matsumoto, *J. Am. Ceram. Soc.* **74,** 1459 (1991).
26. L. Bonhomme-Coury, N. Lequeux, S. Mussotte, and P. Bloch, *J. Sol–Gel Sci. Technol.* **2,** 371 (1994).